Sukrungsri and Pailoplee *Earth, Planets and Space*
DOI 10.1186/s40623-015-0269-0

Earth, Planets and Space
a SpringerOpen Journal

FULL PAPER Open Access

# Precursory seismicity changes prior to major earthquakes along the Sumatra-Andaman subduction zone: a region-time-length algorithm approach

Santawat Sukrungsri and Santi Pailoplee*

**Abstract**

In this study, we investigated the precursory seismicity changes related to the major earthquakes posed along the Sumatra-Andaman subduction zone (SASZ) using the region-time-length (RTL) algorithm. Based on the suitable RTL characteristics of $r_0$ = 100 km and $t_0$ = 2 years, the anomalous RTL score representing the quiescence stage mostly started 0.1–5.2 years before the subsequent major earthquake, while no activation stage was illustrated. For the spatial investigation, the RTL anomalies also clearly illustrated the location of the subsequent major earthquakes. Thus, in order to determine the prospective areas of upcoming earthquakes, the series of RTL maps calculated during the recent 5-year (2010–2014) time span was used. The obtained results reveal four risk areas along the SASZ that might pose a major earthquake in the future, namely (i) Sittwe city, western Myanmar; (ii) offshore northern Nicobar Islands; (iii) Aceh city, northernmost of Sumatra Island; and (iv) offshore western Sumatra Island. Therefore, both a tsunami hazard in the Indian Ocean and a seismic hazard in the far-field cities should be recognized urgently.

**Keywords:** Seismicity; RTL algorithm; Quiescence; Precursor; Sumatra-Andaman subduction zone

## Background

The present-day activities of the Indian-Eurasian plate collision, the plate boundary called the Sumatra-Andaman subduction zone (SASZ), have caused frequent hazardous earthquakes (Fig. 1; Pailoplee and Choowong 2014). In addition, not only was the last tsunami originated by a $M_w$-9.0 earthquake on December 26th, 2004 but also paleotsunami evidence supports that the SASZ is a significant tsunamogenic source (Jankaew et al. 2008; Monecke et al. 2008). Geographically, the tsunami hazard created here impacts upon a number of countries surrounding the Indian Ocean. Such far-field SASZ earthquakes normally generate long-period ground motions that directly effect tall buildings and in particular in Bangkok, the capital city of Thailand. Hence, some researchers have attempted to clarify the seismogenic situation along the SASZ.

Using statistical seismology, the possibility of applying the frequency-magnitude distribution (FMD; Gutenberg and Richter 1944) model as an earthquake precursor was demonstrated along the SASZ (e.g., Nuannin et al. 2005; Pailoplee and Choowong 2014). In particular, utilizing the 50 closest earthquakes in an individual site of interest, Nuannin et al. (2005) found that a low-FMD b-value was related to a high accumulated tectonic stress and so implied a prospective area of upcoming earthquakes. Thereafter, using Nuannin et al.'s (2005) assumption, the comparative low-FMD b-value areas along the northern segment of the SASZ were evaluated, revealing that (i) Sittwe city, western Myanmar, and (ii) offshore northern Nicobar Islands might be subject to strong-to-major earthquakes soon (Pailoplee et al. 2013). However, up to 2014, all the seismic

* Correspondence: Pailoplee.S@gmail.com
Earthquake and Tectonic Geology Research Unit (EATGRU), Department of Geology, Faculty of Science, Chulalongkorn University, Bangkok 10330, Thailand

risk areas mentioned above are still quiescent and so should be monitored carefully.

Since the existence of quiescent and activation stages of earthquakes was reported (Sobolev 1995), an alternative statistical method called the region-time-length (RTL) algorithm was developed to investigate such stages of seismicity (Sobolev and Tyupkin 1997, 1999). As a result of extended practice, a number of RTL investigations have revealed the successful correlation between the quiescent and/or activation stages and the subsequent moderate-to-major earthquakes in various seismogenic settings, such as the $M_w$-7.2 Kobe earthquake, Japan (Huang et al. 2001), $M_w$-6.8 Nemuro earthquake, Japan (Huang and Sobolev 2002), $M_w$-7.3 Izmit earthquake, Turkey (Huang et al. 2002), $M_S$-7.3 Tottori earthquake, Japan (Huang and Nagao 2002), earthquakes with $M_S \geq 5.0$ in northern China (Jiang et al. 2004), earthquakes with $M_S \geq 6.0$ in the Yunnan area (Liu and Su 2006), $M_w$-7.3 Chi-Chi earthquake, Taiwan (Chen and Wu 2006), $M_S$-8.0 Wenchuan earthquake, China (Huang 2008), and the latest hazardous event of the $M_w$-9.0 Tohoku earthquake, Japan (Huang and Ding 2012). In order to constrain the prospective earthquake sources proposed previously by Pailoplee et al. (2013), the RTL algorithm was applied in this study to the most up-to-date seismicity data recorded along the SASZ.

## Methods

The RTL algorithm weights simultaneously the functions of distance ($R(x,y,z,t)$), time ($T(x,y,z,t)$) and rupture length ($L(x,y,z,t)$), as expressed in Eqs. (1–3), respectively (Sobolev and Tyupkin 1997, 1999):

$$R(x,y,z,t) = \left[\sum_{i=1}^{n} \exp\left(-\frac{r_i}{r_0}\right)\right] - R_{bg}(x,y,g,t), \quad (1)$$

$$T(x,y,z,t) = \left[\sum_{i=1}^{n} \exp\left(-\frac{t-t_i}{t_0}\right)\right] - T_{bg}(x,y,z,t), \quad (2)$$

$$L(x,y,z,t) = \left[\sum_{i=1}^{n} \exp\left(-\frac{l_i}{r_i}\right)\right] - L_{bg}(x,y,z,t), \quad (3)$$

where ($x,y,z,t$) are the investigated site and time, $t_i$ and $l_i$ are the origin time and rupture length of the $i$th considered earthquake and $r_i$ is the distance between the investigated site and earthquake focus. For the SASZ region, the rupture length was given by the empirical relationship between the rupture length and earthquake magnitude ($M_i$), based mainly on Papazachos et al.'s (2004) assumption. Meanwhile, $r_0$ and $t_0$ are the characteristic distance and time span, respectively. The $R_{bg}(x,y,z)$, $T_{bg}(x,y,z)$, and $L_{bg}(x,y,z)$ are the background values of $R(x,y,z)$, $T(x,y,z)$, and $L(x,y,z)$, respectively, and $n$ is the number of earthquakes satisfying some criteria, as shown in Eqs. (4–6):

$$M_i \geq M_c, \quad (4)$$

$$r_i \leq R_{max} = 2r_0, \quad (5)$$

$$t_i \leq T_{max} = 2t_0. \quad (6)$$

In order to limit the variations of the obtained weighting, the RTL score ($V_{RTL}(x,y,z,t)$) was evaluated and normalized as in Eq. (7).

$$V_{RTL}(x,y,z,t) = \frac{R(x,y,z,t)}{R(x,y,z,t)_{max}} \cdot \frac{T(x,y,z,t)}{T(x,y,z,t)_{max}} \cdot \frac{L(x,y,z,t)}{L(x,y,z,t)_{max}} \quad (7)$$

According to Eq. (7), the RTL score varies between −1 and 1, where a RTL score of <0 or >0 implies a quiescent or activation stage, respectively, when the background RTL score = 0.

## Results and discussion

### Dataset and completeness

The seismicity data compiled by the (i) International Seismological Center, (ii) US National Earthquake Information Center, and (iii) Global Centroid Moment Tensor were used in this study. Together, these datasets recorded a total of 104,780 earthquake events along the SASZ during 1964–2014. In order to investigate only the interplate activities of the SASZ, the earthquakes with a depth >45 km, defined as the subducting slab, were excluded. The earthquake magnitudes were in the range of 1.7–9.0 but were reported in the different magnitude scales of the body-wave ($m_b$), surface-wave ($M_S$), and moment ($M_w$) magnitudes. Therefore, the different magnitude scales were homogenized to $M_w$ using the empirical relationships contributed by the Global Centroid Moment Tensor data available along the SASZ (Fig. 2a, b).

Using the assumption suggested by Gardner and Knopoff (1974), 102,017 events of earthquakes were defined as dependent foreshocks or aftershocks and so were eliminated. The completeness of the earthquake-detecting procedure was checked using the FMD power-law. Based on the assumption of the entire-magnitude range (Woessner and Wiemer 2005), a magnitude of completeness (Mc) of $M_w$-4.6 was found to cover most parts of the SASZ (Fig. 2c).

In addition, by recognizing the GENAS algorithm (Habermann 1983, 1987), the mainshock data was found to have a consistent seismicity with $M_w \geq 4.6$ during 1980–2014. The straight line of the cumulative number of earthquakes (Fig. 2d) indicates no obvious man-made change in the bulk seismicity rate (Wyss 1991; Zuniga

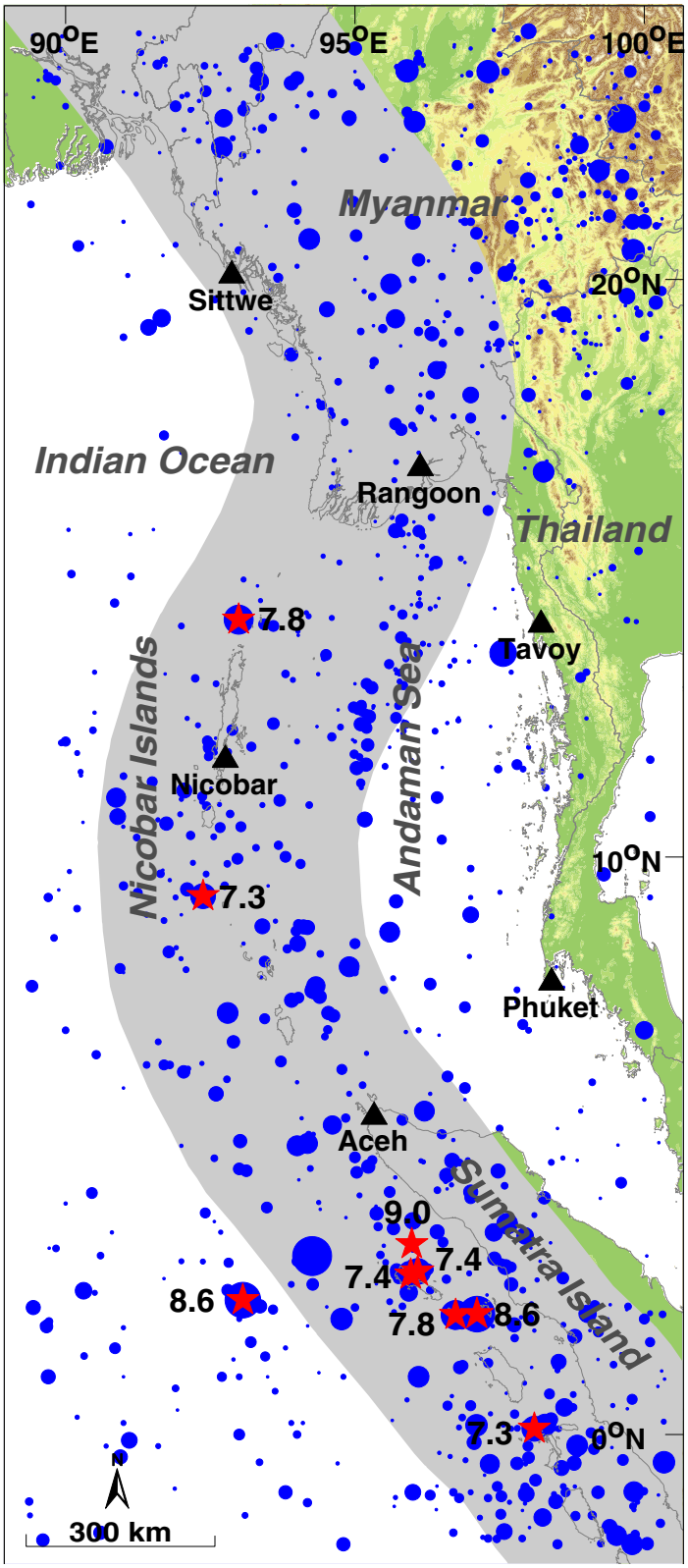


**Fig. 1** Map of the Sumatra-Andaman subduction zone (SASZ; *grey polygon*) and the adjacent areas showing the epicentral distributions of the completeness mainshocks with a $M_w \geq 4.6$ recorded during 1980–2014. The *red stars* are the major earthquakes with $M_w \geq 7.0$

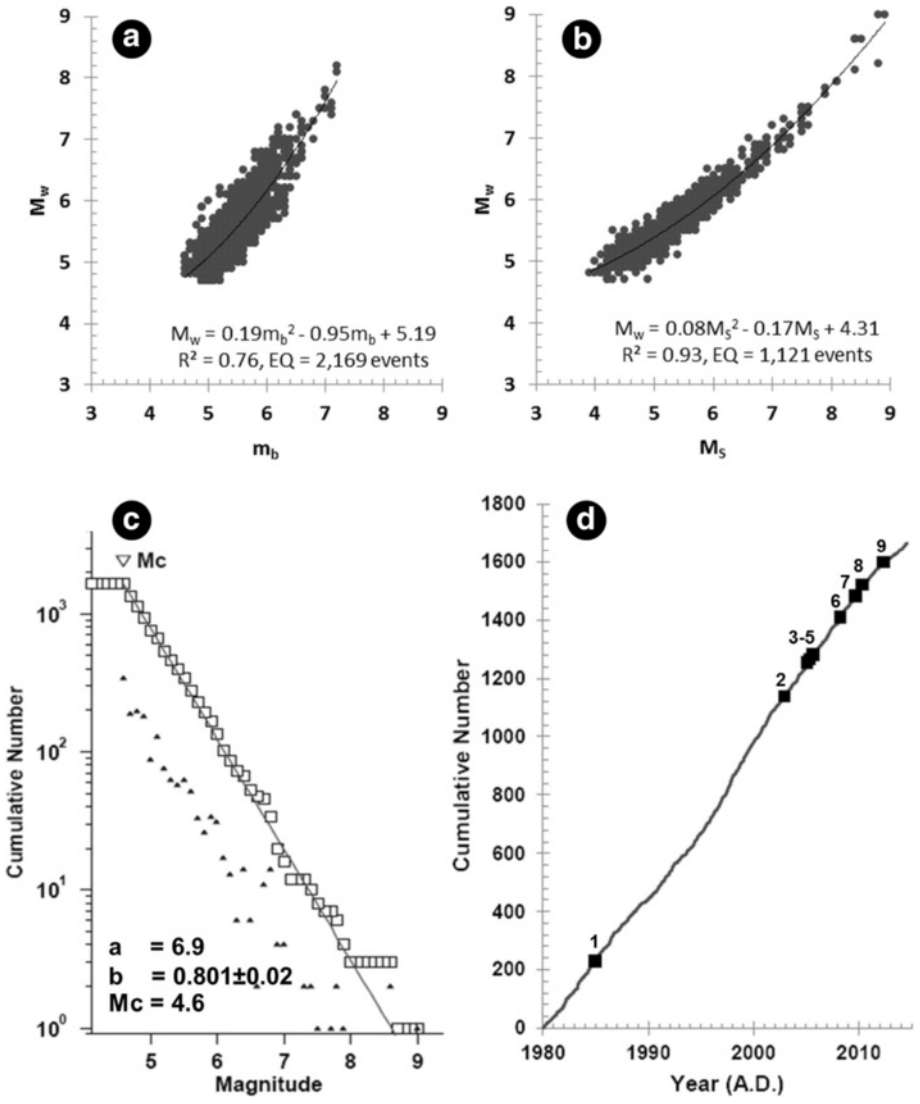


**Fig. 2** Empirical relationships of **a** $M_w$-$m_b$ and **b** $M_w$-$M_S$. The best fit regression line, its equation, and $R^2$ value are shown. **c** FMD plots of the mainshocks reported along the SASZ. *Triangles* indicate the number of earthquakes of each magnitude and *squares* represent the cumulative number of earthquakes equal to or larger than each magnitude. *Solid lines* are the lines of best fit according to Woessner and Wiemer (2005). **d** Cumulative number of mainshocks with $M_w \geq 4.6$ detected during 1980–2014. *Black squares* are the major earthquakes with $M_w \geq 7.0$. The number mentioned above each square is equivalent to the "No." column in Table 1

and Wiemer 1999). Therefore, all of the remaining 1668 mainshocks with a $M_w \geq 4.6$ recorded during 1980–2014 were used in this RTL investigation.

## Retrospective investigation

In order to (i) test the potential of the RTL algorithm as a reliable marker of an earthquake precursor and (ii) find out the suitable RTL characteristics of $r_0$ and $t_0$ corresponding to $R_{max}$ and $T_{max}$, nine major earthquakes that occurred along the SASZ during 1980–2014 (Table 1) were investigated retrospectively using the RTL algorithm. The parameter $R_{max}$ was varied between 50 and 250 km with a 10-km space window, while $T_{max}$ was evaluated between 0.5 and 10.5 years with a 0.5-year time window. Thus, in total, 400 (20 × 20) characteristic conditions were tested iteratively.

### *Temporal investigation*

In each epicenter of the demonstrated earthquake (Table 1), the RTL score was calculated every 14 days starting from 1980 up to the recorded occurrence of the earthquake. According to these iterative tests, values of $R_{max}$ = 200 km and $T_{max}$ = 4 years, i.e., $r_0$ = 100 km and $t_0$ = 2 years, allowed detection of the anomalous drop in the RTL score prior to the occurrence of all recognized earthquakes (Fig. 3). The minimum RTL score varied

**Table 1** List of earthquake events with $M_w \geq 7.0$ posed along the SASZ during 1980–2014

| No. | Longitude (degree) | Latitude (degree) | Depth (km) | Date | Time | Magnitude ($M_w$) |
|---|---|---|---|---|---|---|
| 1. | 98.10 | 0.10 | 34 | 17/11/1984 | 06:49 | 7.3 |
| 2. | 96.09 | 2.82 | 30 | 02/11/2002 | 01:26 | 7.4 |
| 3. | 95.98 | 3.30 | 30 | 26/12/2004 | 00:58 | 9.0 |
| 4. | 97.11 | 2.09 | 30 | 28/03/2005 | 16:09 | 8.6 |
| 5. | 92.38 | 9.32 | 16 | 24/07/2005 | 15:42 | 7.3 |
| 6. | 95.96 | 2.77 | 26 | 20/02/2008 | 8:08 | 7.4 |
| 7. | 92.99 | 14.11 | 10 | 10/08/2009 | 19:55 | 7.8 |
| 8. | 96.74 | 2.07 | 18 | 06/04/2010 | 22:15 | 7.8 |
| 9. | 93.06 | 2.33 | 20 | 11/04/2012 | 08:38 | 8.6 |

between −0.13 (Fig. 3d) and −0.96 (Fig. 3i) and were mostly more than −0.5 lower than the minimum RTL score, i.e., −1. This indicates that the anomalous drop in the RTL score was fairly obvious as a quiescence precursor. However, in this study, no prominent evidence of the activation stage was found, as has also been mentioned previously for the $M_w$-7.2 Kobe earthquake, Japan (Huang et al. 2001), $M_w$-6.8 Nemuro earthquake, Japan (Huang and Sobolev 2002), and $M_w$-7.3 Chi-Chi earthquake, Taiwan (Chen and Wu 2006).

Although only 4 years of seismicity data (1980–1984) were used, the graph illustrates a significant drop in the RTL score at 1984.69 followed by the $M_w$-7.3 earthquake in November 17th, 1984 (Fig. 3a). In the case of the devastating $M_w$-9.0 earthquake at the end of 2004, the quiescence stage was evident from 2002.56 and reached its minimum RTL value (−0.58) at 2002.87 (Fig. 3c).

Regarding the time span between the occurrences of an anomalous RTL score and subsequent major earthquakes, most case studies illustrated a short time period of 0.1–5.2 years (Fig. 3a–h). This indicates that monitoring of the RTL measurements with $r_0$ = 100 km and $t_0$ = 2 years may be useful for the intermediate-term (months, years) earthquake forecasting along the SASZ. Although the RTL anomalies appear almost 15 years before the $M_w$-8.6 earthquake of 2012, the calculated RTL score dropped obviously to −0.96 in mid-1997 (Fig. 3i).

In order to examine the reliability of utilized characteristic parameters, both $r_0$ and $t_0$ were varied (Table 2), and the RTL score at the epicenter of the $M_w$-9.0 earthquake was investigated temporally (Fig. 4a). The correlation coefficients of each varied $r_0$ and $t_0$ parameter compared to the utilized $r_0$ = 100 km and $t_0$ = 2 year values, respectively, were also evaluated, and the results are summarized in Table 2. Based on Huang (2005), the correlation coefficients that ranged between 0.81 and 0.91 indicated that all the varied cases listed in Table 2 correlated at a significance of 0.05. As a result, one can conclude that the values of $r_0$ = 100 km and $t_0$ = 2 years utilized in this study are meaningful for RTL investigation along the SASZ and that the seismic quiescence obtained here is not an artifact due to parameter selections.

### *Spatial investigation*

In order to constrain the potential of the RTL algorithm for intermediate-term earthquake forecasting, the spatial distribution of the RTL score was also evaluated in this study. At first, the area in the vicinity of SASZ was gridded with a 0.25° × 0.25° spacing, and the temporal variations of RTL scores were evaluated in each grid node. Thereafter, an average of the RTL score ($Q(x,y,z,t_1,t_2)$) at each grid node ($x,y,z$) over the time span of interest ($t_1,t_2$) was determined systematically as reported (Huang et al. 2002) according to Eq. (8):

$$Q(x,y,z,t_1,t_2) = \frac{1}{m}\sum_{i=1}^{m} V_{\mathrm{RTL}}(x,y,z,t), \tag{8}$$

where $m$ is the number of RTL score data available in the time span $t_1$ to $t_2$.

The spatial distribution of the average RTL score in the individual time spans of interest for the nine major earthquakes revealed that all these earthquakes were generated in the vicinity of a comparatively low RTL score (Fig. 5). For example, prior to the $M_w$-7.3 earthquake of November 17th, 1984, at the offshore western Sumatra Island, an anomalous RTL score was evident 0.15 years during 1984.69–1984.84 (Fig. 5a). However, according to the short utilized seismicity data mentioned above, some additional anomalies are also shown in the other regions of Sittwe city and southern Nicobar Islands (Fig. 5a).

The RTL maps still illustrated clearly the anomalies at the offshore western Sumatra Island (Fig. 5b, c), where the anomalous RTL score seen 0.19 years during 1997.46–1997.65 was followed by the $M_w$-7.4 earthquake on November 2nd, 2002 (Fig. 5b) and the $M_w$-9.0 earthquake of December 26th, 2004, followed 0.12 years of

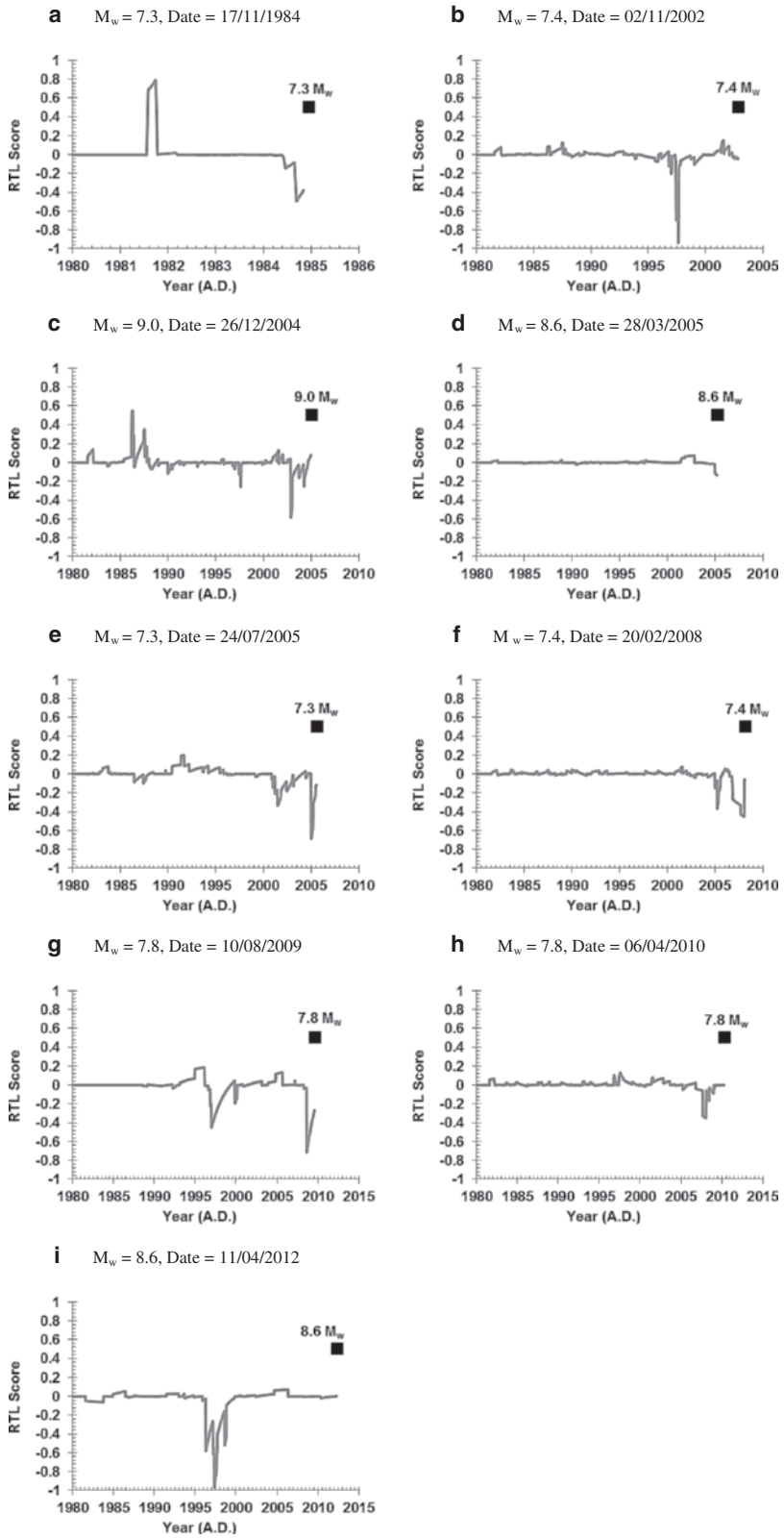


**Fig. 3** Temporal variations in the RTL score at the individual epicenter of each of the nine major earthquakes recognized in the retrospective RTL investigation. **a** $M_W$-7.3 in 1984, **b** $M_W$-7.4 in 2002, **c** $M_W$-9.0 in 2004, **d** $M_W$-8.6 in 2005, **e** $M_W$-7.3 in 2005, **f** $M_W$-7.4 in 2008, **g** $M_W$-7.8 in 2009, **h** $M_W$-7.8 in 2010, and **i** $M_W$-8.6 in 2012. The *black squares* indicate the occurrence time of each major earthquake

**Table 2** Correlation coefficients of the RTL values between different characteristic parameters $r_0$ and $t_0$

| Case A | $r_0$ = 100 km, $t_0$ = 2 years | | | |
|---|---|---|---|---|
| Case B | $r_0$ = 75 km | $r_0$ = 125 km | $t_0$ = 1.75 years | $t_0$ = 2.25 years |
| Correlation of A and B | 0.82 | 0.91 | 0.81 | 0.81 |

the anomalous RTL score during 2002.87–2002.99 (Fig. 5c). During 2005, two RTL anomalies were evident along the SASZ, where the average RTL score decreased down to −0.3 to −0.8 during 2005.02–2005.44 followed by the $M_w$-8.6 and $M_w$-7.3 earthquakes on March 28th and July 24th of 2005 at the southern Nicobar Islands and the offshore western Sumatra Island, respectively (Fig. 5d, e).

Moreover, there were two additional precursory RTL scores that could be observed at the offshore western Sumatra Island during 2006.86–2008.05 (1.19 years) and 2007.70–2008.05 (0.35 years) (Fig. 5f, h), which were followed by earthquakes of $M_w$-7.4 and $M_w$-7.8 on February 20th, 2008 and April 6th, 2010, respectively. Meanwhile, for the offshore northern Nicobar Islands, the $M_w$-7.8 earthquake of August 10th, 2009, was within 1 year of the prominent RTL anomalies seen during 2008.62–2009.58 (Fig. 5g). For the latest major earthquake of the SASZ, only one obvious RTL anomaly was detected 0.23-year long during 1997.35–1997.58, and this preceded the $M_w$-8.6 earthquake of April 11th, 2012 (Fig. 5i). To test the statistical significance of the obtained RTL anomalies, the earthquake data were synthesized randomly in the study area according to stochastic process (Huang et al. 2002). Thereafter, the RTL anomalies at nine epicenters of the major earthquakes demonstrated here were evaluated. From 10,000 iterative tests with random data, it was revealed that almost all the anomalies obtained here did not result from a stochastic process (Fig. 4b). According to both the temporal and spatial relationship between the origin time and location of the precursory RTL score and the subsequent major earthquakes described above, we preferred and applied the condition of $r_0$ = 100 km and $t_0$ = 2 years for the present-day investigation of the RTL algorithm as shown in the next section (the "Present-day investigation" section).

### Present-day investigation

Based on the suitable values of $r_0$ and $t_0$ obtained from the retrospective test, we then investigated the spatial distribution of the RTL anomalies for the most up-to-date seismicity data (2010–2014). As a result, four small areas showed noticeable RTL anomalies in different time spans. At Sittwe city, western Myanmar, the anomalous

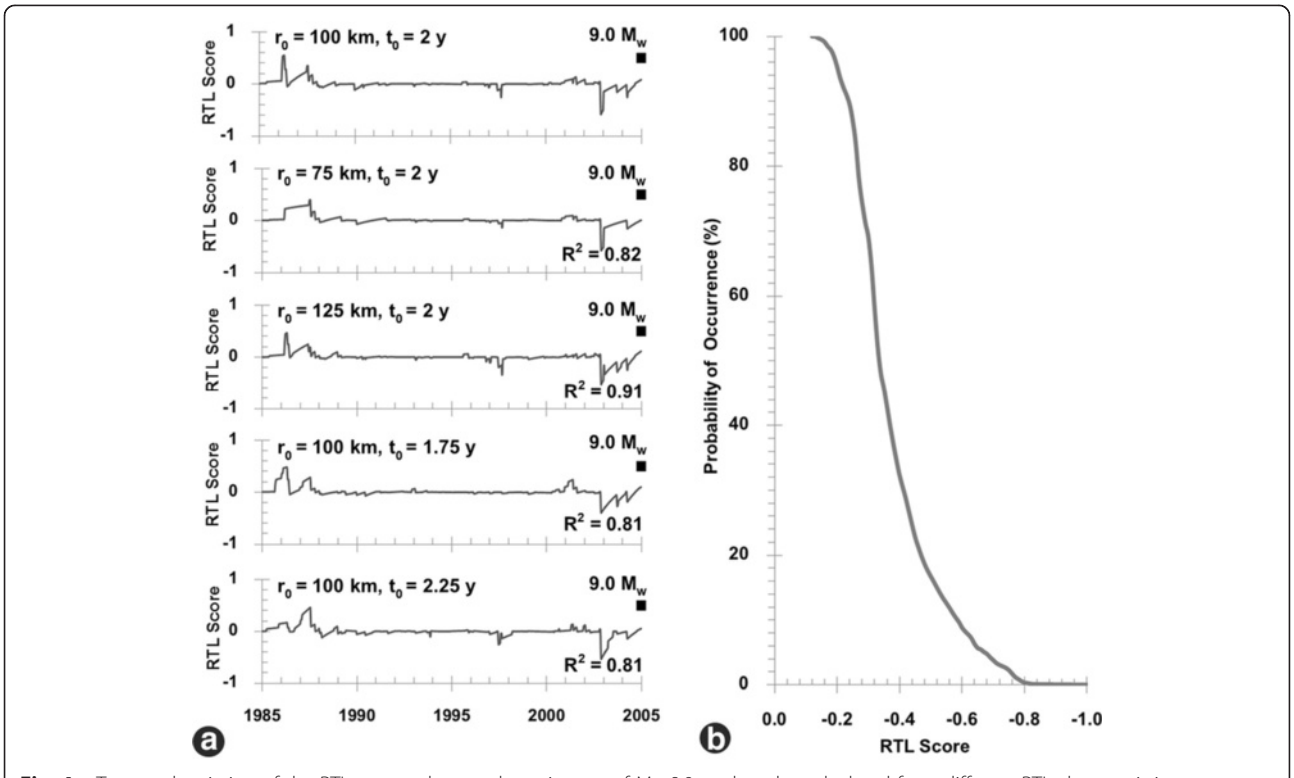


**Fig. 4 a** Temporal variation of the RTL scores, close to the epicenter of $M_w$-9.0 earthquake, calculated from different RTL characteristic parameters. Right side below corner of each curve is the value of correlation coefficient with curve. **b** The probability of occurrence (%) in each level RTL score at the epicenter of $M_w$-9.0 earthquake evaluated from the random earthquake data

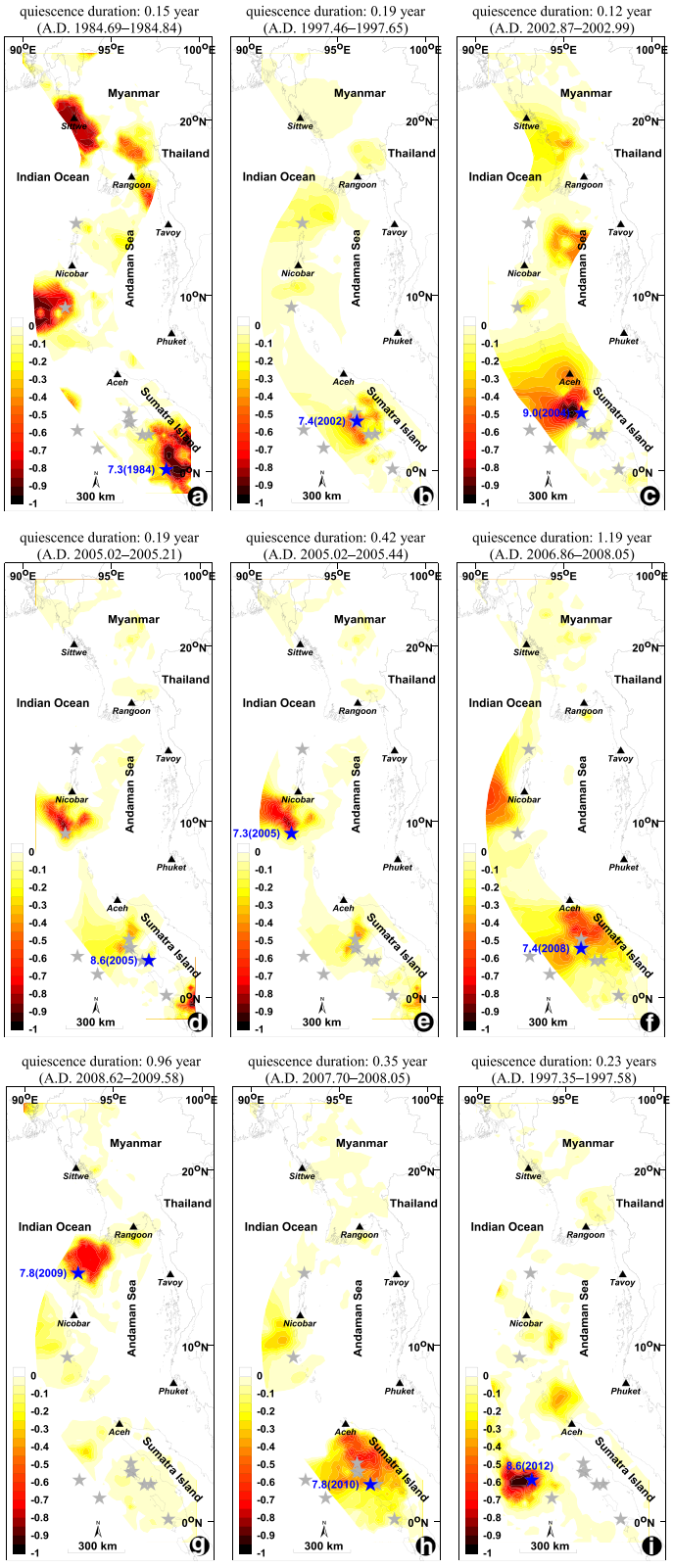


**Fig. 5** Spatial distributions of the average RTL scores determined in the individual period of interest. **a** 1984.69–1984.84, **b** 1997.46–1997.65, **c** 2002.87–2002.99, **d** 2005.02–2005.21, **e** 2005.02–2005.44, **f** 2006.86–2008.05, **g** 2008.62–2009.58, **h** 2007.70–2008.05, and **i** 1997.35–1997.58. The *blue stars* represent the epicenters of the subsequent major earthquakes

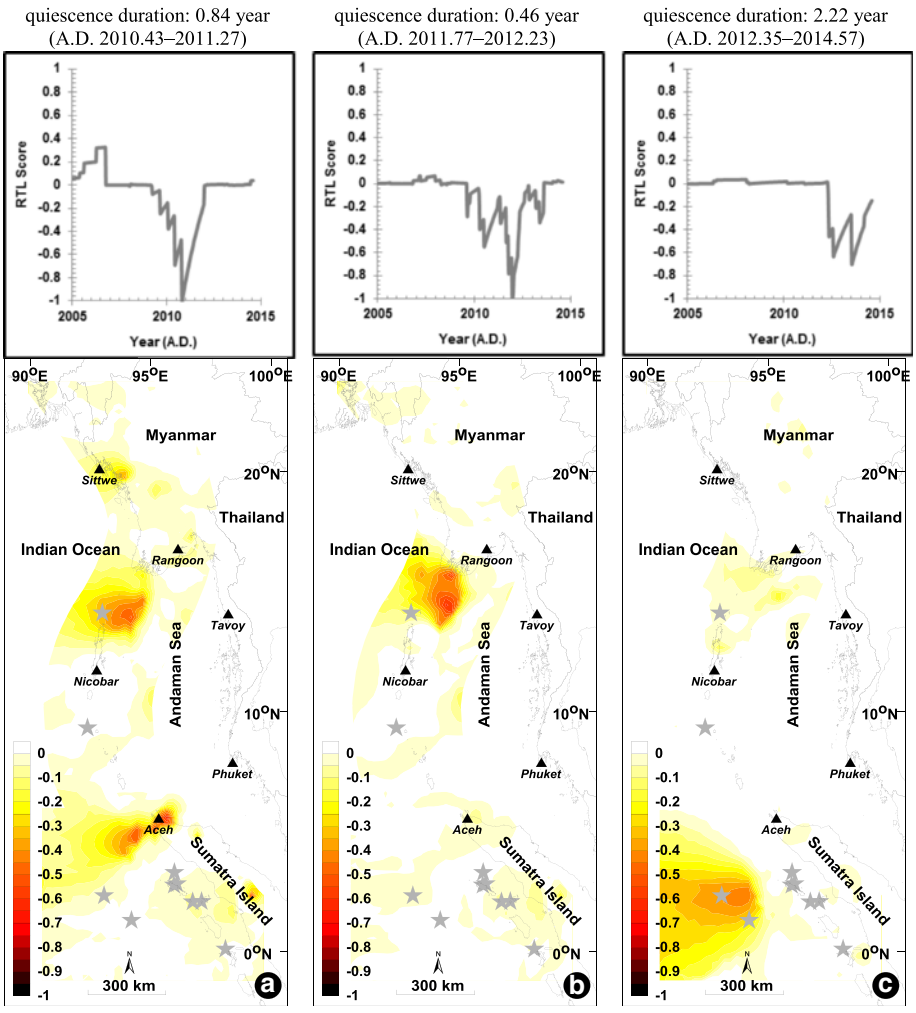


**Fig. 6** Temporal and spatial distributions of the average RTL scores determined during 2010–2014. **a** 2010.43–2011.27, **b** 2011.77–2012.23, and **c** 2012.35–2014.57

RTL score appeared for just under 1 year during 2010.43–2011.27 (Fig. 6a), while for the offshore northern Nicobar Islands, the anomalies existed for almost 2 years during 2010.43–2012.23 (Figs. 5b and 6a).

Based on the FMD investigation using the seismicity data until 2010, Pailoplee et al. (2013) proposed two prospective areas of upcoming earthquakes, namely at Sittwe city and the offshore northern Nicobar Islands. This study, using the anomalous RTL values, concurs with the previous work of Pailoplee et al. (2013) and supports the high possibility of a major earthquake soon at Sittwe city and the northern Nicobar Islands.

In addition, it should be mentioned that other intense RTL anomalies were also detected around (i) Aceh city, northernmost of Sumatra Island, and (ii) offshore western Sumatra Island during 2010.43–2011.27 and 2012.35–2014.57, respectively (Figs. 5c and 6a). No significant earthquakes have been reported in the vicinity of these two regions since 2012, and so, these regions are additionally proposed as being high seismic risk areas that are likely to experience an earthquake in the near future.

## Conclusions

We investigated retrospectively the seismicity changes prior to nine major earthquakes generated along the SASZ by applying the RTL algorithm with the completeness earthquake catalogue. Based on this iterative test, suitable $r_0$ (100 km) and $t_0$ (2 years) values were found and led the RTL algorithm to illustrate the meaningful quiescence anomalies prior to the occurrence of all nine major earthquakes, although no activation stage was prominent. For the duration between the detectable RTL anomalies and the subsequent major earthquakes, quiescence was most frequently detected in the range of 0.1–5.2 years before the earthquake, which provides the best

opportunity for the application of this RTL algorithm to intermediate-term earthquake forecasting at the SASZ region. As a result, we also evaluated the spatial variations of the RTL anomalies with the most up-to-date seismicity data (2010–2014) and concluded that there are four regions that have a possibility to generate a major earthquake in the near future (Fig. 6). These were (i) Sittwe city, western Myanmar, (ii) offshore northern Nicobar Islands, (iii) Aceh city, northernmost of Sumatra Island, and (iv) offshore western Sumatra Island. Therefore, effective mitigation plans for both seismic and tsunami hazards should be developed and implemented.

**Competing interests**
The authors declare that they have no competing interests.

**Authors' contributions**
SS carried out the data preparation, data improvement, and seismicity investigations. SP performed the statistical analysis, design of the study, and the sequence alignment, including drafting of the manuscript. Both authors read and approved the final manuscript.

**Acknowledgements**
This research was supported by the Ratchadapiseksomphot Endowment Fund 2015 of Chulalongkorn University (WCU-58-021-CC). Thanks are also extended to T. Pailoplee for the preparation of the draft manuscript. I thank the Publication Counseling Unit (PCU), Faculty of Science, Chulalongkorn University, for a critical review and improved English. I acknowledge thoughtful comments and suggestions by the editors and anonymous reviewers that enhanced the quality of this manuscript significantly.

Received: 23 February 2015 Accepted: 10 June 2015
Published online: 23 June 2015

**References**

Chen C, Wu Y (2006) An improved region-time-length algorithm applied to the 1999 Chi-Chi, Taiwan earthquake. Geophys J Int 166:144–147
Gardner JK, Knopoff L (1974) Is the sequence of earthquakes in southern California, with aftershocks removed, Poissonian? Bull Seismol Soc Am 64(1):363–367
Gutenberg B, Richter CF (1944) Frequency of earthquakes in California. Bull Seismol Soc Am 34:185–188
Habermann RE (1983) Teleseismic detection in the Aleutian Island Arc. J Geophys Res 88:5056–5064
Habermann RE (1987) Man-made changes of seismicity rates. Bull Seismol Soc Am 77:141–159
Huang Q (2005) A method of evaluating reliability of earthquake precursors. Chin J Geophys 48(3):701–707
Huang Q (2008) Seismicity changes prior to the Ms8.0 Wenchuan earthquake in Sichan, China. Geophys Res Lett 35, L23308
Huang Q, Ding X (2012) Spatiotemporal variations of seismic quiescence prior to the 2011 M 9.0 Tohoku Earthquake revealed by an improved region–time–length algorithm. Bull Seismol Soc Am 102(4):1878–1883
Huang Q, Nagao T (2002) Seismic quiescence before the 2000 M=7.3 Tottori earthquake. Geophys Res Lett 29(12):1578
Huang Q, Sobolev GA (2002) Precursory seismicity changes associated with the Nemuro Peninsula earthquake, January 28, 2000. J Asian Earth Sci 21(2):135–146
Huang Q, Sobolev GA, Nagao T (2001) Characteristics of the seismic quiescence and activation patterns before the M=7.2 Kobe earthquake, January 17, 1995. Tectonophysics 337(1–2):99–116
Huang Q, Oncel AO, Sobolev GA (2002) Precursory seismicity changes associated with the $M_w$=7.4 1999 August 17 Izmit (Turkey) earthquake. Geophys J Int 151(1):235–242
Jankaew K, Atwater BF, Sawai Y, Choowong M, Charoentitirat T, Martin ME, Prendergast A (2008) Medieval forewarning of the 2004 Indian Ocean tsunami in Thailand. Nature 455:1228–1231
Jiang H-K, Hou H-F, Zhou H-P, Zhou C-Y (2004) Region-time-length algorithm and its application to the study of intermediate-short term earthquake precursor in North China. Acta Seismol Sin 17(2):164–176
Liu H, Su Y-J (2006) Application of region-time-length algorithm to Yunnan area. J Seismol Res 29(1):25–29
Monecke K, Finger W, Klarer D, Kongko W, McAdoo BB, Moore AL, Sudrajat SU (2008) A 1,000-year sediment record of tsunami recurrence in northern Sumatra. Nature 455:1232–1234
Nuannin P, Kulhánek O, Persson L (2005) Spatial and temporal b-value anomalies preceding the devastating off coast of NW Sumatra earthquake of December 26, 2004. Geophys Res Lett 32, L11307
Pailoplee S, Choowong M (2014) Earthquake frequency–magnitude distribution and fractal dimension in Mainland Southeast Asia. Earth Planets Space 6(8):1–10
Pailoplee S, Surakiatchai P, Charusiri P (2013) b-value Anomalies along the northern segment of Sumatra-Andaman Subduction Zone: Implication for the upcoming earthquakes. J Earthq Tsunami 7(3): 1350030–1–8
Papazachos BC, Scordilis EM, Panagiotopoulos DG, Papazachos CB, Karakaisis GF (2004) Global relations between seismic fault parameters and moment magnitude of earthquakes. Bull Geol Soc Greece 36:1482–1489
Sobolev GA (1995) Fundamental of earthquake prediction. Electromagnetic research center, Moscow, 162 p
Sobolev GA, Tyupkin YS (1997) Low-seismicity precursors of large earthquakes in Kamchatka. Volc Seismol 18:433–446
Sobolev GA, Tyupkin YS (1999) Precursory phases, seismicity precursors, and earthquake prediction in Kamchatka. Volc Seismol 20:615–627
Woessner J, Wiemer S (2005) Assessing the quality of earthquake catalogues: estimating the magnitude of completeness and its uncertainty. Bull Seismol Soc Am 95(2):684–698
Wyss M (1991) Reporting history of the central Aleutians seismograph network and the quiescence preceding the 1986 Andreanof Island earthquake. Bull Seismol Soc Am 81:1231–1254
Zuniga FR, Wiemer S (1999) Seismicity patterns: are they always related to natural causes? Pageoph 155:713–726